Capacitive Biosensing Technique for the Detection of DNA Modification and Hybridization Process Using Custom-made Gold Interdigital Microelectrode Arrays

Nadja E. Solis-Marcano[1], Marjorie Lopez-Nieves[2], Brismar Pinto-Pacheco[3] and Carlos R. Cabrera[4]

Department of Chemistry, Molecular Sciences Research Center, University of Puerto Rico, Rio Piedras Campus, San Juan, PR, 00931

Interest in miniaturized bio-sensing techniques has grown in the past decades for the rapid and accurate detection of disease-causing agents. Innovative custom microdevices provide a greener approach by reducing the cost and waste in terms of sample amount, reagent volumes, size, time and human resources. This is particularly important for outer space environment where timing is crucial and laboratory facilities are not available. Here, we propose a non-faradaic, label-free, electrochemical method based on capacitance measurement to sense DNA surface modification and hybridization. We created custom-made gold interdigital microelectrodes arrays using photolithography technique. Silver electroplating was used to make a stable silver silver/chloride quasi-reference electrode. Self assembled monolayers of B. Anthracis aptamer at two different surface coverage were made and exposed to complementary, non-complementary and mismatch strands to study the hybridization and/or non-hybridization processes by means of double layer capacitance (C_{dl}) measurements at two given applied potentials using Electrochemical Impedance Spectroscopy (EIS) analysis. An average percentage change in C_{dl} of 31.0% and 19.8% were obtained for the low and high Anthracis aptamer coverage respectively when exposed to its complementary target. The conditions that showed better distinction between strand interactions, as well as lower error bars, were low surface coverage at 0.3V vs. E_{oc} applied potential. Overall results showed that double layer capacitance is a measurable property to detect specific DNA sequences.

Nomenclature

C_{dl}	=	double layer capacitance
EIS	=	electrochemical impedance spectroscopy
V	=	volts
MS	=	Mass Spectrometer
PZC	=	zero charge potential
ssDNA	=	single strand DNA
dsDNA	=	double strand DNA
MES	=	2-ethanesulfonic acid
NaCl	=	sodium chloride
H_2SO_4	=	sulfuric acid
MCH	=	6-mercapto-1-hexanol
E_{oc}	=	open circuit potential
EDS	=	energy dispersive spectroscopy
SEM	=	scanning electron microscopy
R_s	=	solution resistance
R_{ct}	=	charge transfer resistance

[1] Department of Chemistry, nadja.enid@gmail.com
[2] Department of Interdisciplinary, marjorielopeznieves@gmail.com
[3] Department of Chemistry, bpp240@nyu.edu
[4] Department of Chemistry, carlos.cabrera2@upr.edu

I. Introduction

SPACE suitable biosensors have had an increase in demand in the last decade due to the need for rapid, accurate and low-maintenance methods to detect pathogenic bacteria, viruses and other disease causing agents that can put at risk the health of astronauts and space exploration missions.[1] A biosensor is a device composed of a biological recognition element and a transducer that senses and converts a biological response into a measurable signal. Among other bio-recognition components, single stranded DNA, also known as aptamers, have been utilized as bio-receptors in biomedical research for fast and easy diagnostic of diseases since each living organism contains a specific DNA sequence that can be selectively identified.[2]

Conventional DNA hybridization biosensors are made by either labeling using a fluorescent probe to spectroscopically follow the hybridization process due to changes in intensity emitted[3], or by labeling with a redox active molecule that executes an electron exchange when close to an electrode surface[4]. Label-free, faradaic DNA biosensors typically measures faradaic current changes using a redox pair such a $Fe(CN)_6^{3-/4-}$ or $Ru(NH_3)_6^{2+/3+}$ as indicator[5,6]. There also exist a variety of creative DNA biosensors like the one proposed by Q. Sheng, et. al.,[7] in which they created a cocaine biosensor based on the three-dimensional DNA nanostructure conversion from Triangular Pyramid Frustum to Equilateral Triangle monitored electrochemically and microscopically using transmission electron microscope images. Another example is the vertical nano-gap biosensor created by R. L. Zaffino, et. al.[8] which consists of the completion of the circuit created by complementary to both ends target and parallel DNA modified walls that hybridize to close the gap.

Considerable effort has been made to miniaturize and integrate DNA hybridization sensing processes in a reliable and robust microchip. Innovative custom microdevices can improve modern test diagnostics while providing an ecofriendlyer approach by reducing costs in terms of sample amount, reagent volumes, size, time and human resources.[8] Electrochemical based detection methods are suitable for miniaturized real-time point-of-care applications due to its sensitivity, specificity, small power consumption and low cost.[9] Electrochemical impedance spectroscopy (EIS) is an outstanding, non-destructive technique applicable for studying charged surfaces interaction with molecules such as DNA.[10] There are commercially available miniature potentiostats with the ability of performing EIS analysis. This is an advantange that can be of great use for working in extreme enviroments such as outer-space habitats where time is limited and laboratories facilities are not accessible. Characterization of DNA immobilized onto an electrode surface using EIS can be achieved measuring the change in impedimetric response upon hybridization either in terms of kinetics of electron transfer process by faradaic measurements or in terms of alterations of capacitance and molecular layer organization, originating from biorecognition events, by non-faradaic approach[2]. Also, when utilized for impedance analysis, aptamers have shown the advantage of low noise and high repeatability that comes by their small size and uniformity.[11]

Previous research using label-free, non-faradaic methods to sense DNA hybridization has been performed by our research group, although not miniaturized. J. Rivera-Gandía, et. al.[12] managed to detect the double layer capacitance of self-assembled monolayer hairpin probes before and after exposure to complementary strand, at two distinct potentials: zero charge potential (PZC) and a higher voltage positive to PZC. They noted that single stranded DNA (ssDNA) hairpin showed a higher C_{dl} at PZC, while double stranded DNA (dsDNA) showed a higher C_{dl} at the higher voltage.

In this work, we propose a non-faradaic, label-free, electrochemical biosensor microchip for the recognition and detection of specific DNA sequences. Our microchip will sense the double layer capacitance (C_{dl}) changes produced on the microelectrodes surface upon the hybridization process. The use of label-free methods avoids lengthy, complex pre-treatments and unwanted alterations of the samples.[13] Non-faradaic current is generated by processes where direct transfer of electrons to or from the electrode surface does not occur, such as, movement of electrolyte ions and re-orientation of solvent dipoles. Also, additional reagents are not required in non-faradaic experiments, which make them a greener approach and an excellent choice for point-of-care applications.[14]

Anthrax is an infectious disease caused by the intake of the gram-positive, *Bacillus anthracis* bacteria endospores. Currently, anthrax, as well as most bacterial diseases, are diagnosed by performing blood and wound (if present) bacterial cultures.[15] Besides the long hours and materials it takes to perform the culture, the disease must be previously suspected in order to reach this step. Modern methods have been developed to accurately identify bacteria, for example, S. R. Kalb uses Mass Spectrometry (MS) to obtain the bacterial protein "fingerprint", which is unique to each microorganism. Nevertheless, a 12-24 hours culture is needed to obtain a bacterial colony prior measurements,[16] aside from the MS equipment, which is not suitable for space aircraft. There are numerous tecniques and commercially available kits for aircraft-friendly extraction and isolation of DNA, depending on the cells origin source, (e.g. blood, urine, saliva or surfaces) and physical characteristics (e.g. Gram positive or negative) [1,17,18] Although *B. anthracis* bacterial DNA hairpins were utilized in this research, it should be noted that an

important characteristic of our unlabeled, capacitive biosensor is the opportunity of detecting a vast variaety of pathogenic organisms simply by using the corresponding aptamer probe.

II. Experimental Section

A. Materials

2-ethanesulfonic free acid monohydrate (MES) and Sodium Chloride (NaCl) from Sigma-Aldrich were used to prepare the 100 mM MES/1.0 M NaCl buffer solution at pH 6.15. All other reagents were obtained with high grades and used as received. DNA hairpins and targets were purchased from Integrated DNA Technologies Inc. (Skokie, Illinois, USA). Sequences are listed in Table 1. The B. Anthracis probe was ordered with a 5'-SH-$(CH_2)_6$ modifyer to achieve a covalent bonding onto the gold microelectrodes. All oligos were diluted in 1.0 mL nanopure water (18.0 MΩ) and stored at -20°C until use. Since B. Anthracis came with a disulfide protecting group, it was deprotected by diluting in 1.5 mL of a 0.4 M dithiothreitol solution in 0.17 M phosphate buffer at pH 8.0 and left overnight at room temperature. The treated solution was then run through a NAP-10 size exclusion column (GE Healthcare, Buckinghamshire, UK) that has been previously pre-equilibrated with 0.01 M sodium phosphate buffer at pH 6.8 to isolate the deprotected probe and stored at -20°C. BioSpec-nano spectrophotometer (Shimadzu, Kyoto, Japan) was utilized to calculate the concentration of the deprotected stock B. Anthracis probe solution. Further dilutions were made using MES buffer at pH 6.15.

Table 1. Sequences of probes and targets utilized in the analysis. (Underlined bases represent mismatch sites)

Name	Sequence (5' to 3')
B.Anthracis probe	5THIOMC6-D/CCG ACG AGG GTT GTC AGA GGA TGC GTC GG
B.Anthracis target	CCG ACG AGG GTT GTC AGA GGA TGC GTC GG
Complementary target	GGC TGC TCC CAA CAG TCT CCT ACG CAG CC
3-Mismatch target	GGC TGC TGC CAA CTG TCT CCT ACC CAG CC

B. Custom-made Microelectrode Preparation

Custom gold microelectrodes arrays were prepared in the Conte Nanotechnology Clean Room laboratory at the University of Massachusetts at Amherst (UMass, Amherst, Massachusetts, USA) in collaboration with Dr. James J. Watkins. The microelectrode photomask design was drawn with DraftSight software (Dassault Systèmes, Vélizy-Villacoublay, France) and ordered from Front Range Photomask (Palmer Lake, CO, USA). Boron doped silicon wafers were bought from University Wafer (Boston, MA, USA), diameter: 100 mm, orientation:100.

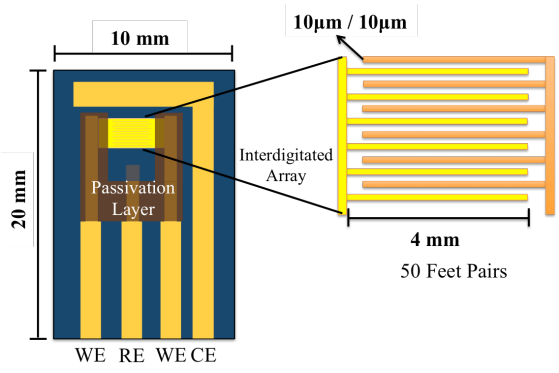

Figure 1. Electrode microchip scheme.

Photolithography was performed as follows: (1) 300 nm silicon dioxide layer was grown onto the wafer using a Vision 310 Plasma Enhanced Chemical Vapor Deposition system (Advance Vacuum, Lomma, Sweden). (2) Shipley 1813 photoresist polymer was coated with a CEE® 100 CB spin coater (Brewer Science Inc., Rolla, MO, USA) and baked at 115 °C for 1 min. (3) Creation of the pattern using the MA6 Mask Aligner equipment (Süss Micro Tech, Garching, Germany) was performed followed by developing in a 4:1 water/351-developer solution and gently dried with a nitrogen flux. (4) SE-600 Electron Beam Evaporator (CHA Industries Inc., Fremont, CA, USA) was used to metalize the surface with a 5 nm titanium layer to enhance the gold adhesion to SiO_2, followed by 150 nm gold deposition. (5) Last step to reveal the microelectrodes chips, lift-off was performed by submerging overnight in acetone. Chip dimensions: 10 mm wide, 20 mm long with four 0.9 mm wide connector bases. Scheme shown in Figure 1, where WE, RE and CE corresponds to the working, reference and counter electrodes, respectively. Working area dimensions: 50

interdigitated feet pairs of 4 mm long, 10 µm wide with 10 µm separation for a total working electrode area of 0.020 cm^2. The microchips were design to fit within a USB port while the posterior part of the cable is stripped and used as contact for the instrument.

Prior use, the wafers were cut into individual microchips and cleaned in a piranha solution for 1 hour. A passivation layer of Kapton® polyimide film (DuPont, Wilmington, DE, USA) was cut by hand and set for 1h at 180°C to restrict the working electrode exposed area. Finally, a silver chloride pseudo reference was created following the silver electrodeposition parameters used by Schlesinger[19] and the chlorination step utilized by Polk[20].

C. Single strand B. Anthracis Immobilization

The microelectrodes were electrochemically cleaned by cycling between 0.100 V – 1.250 V vs. Ag/AgCl, at a scan rate of 50 mV/s in 0.5 M sulfuric acid (H_2SO_4) until a reproducible characteristic clean gold surface voltammogram was obtained. Immobilization of 2.0 µM B. Anthracis hairpin for 2 or 18 hours was performed to study the effect of low and high surface coverages, respectively. Subsequently, the electrodes were rinsed with MES buffer and immobilized with a 10 mM 6-mercapto-1-hexanol (MCH) in DNAse free water solution for 1h to create a mix-monolayer and remove non-specifically adsorbed DNA. Finally, the chip was rinsed with MES buffer and placed in the electrochemical cell arrangement for EIS analysis.

D. Detection

A VMP3 Potentiostat/Galvanostat/EIS (Bio-Logic, USA) was utilized to perform all electrochemical analysis. The frequency range used for EIS ranged from 10,000 – 0.05 Hz, with sinus amplitude of 20 mV and an applied potential of 0.0 and 0.3 V vs. open circuit potential (E_{oc}). Impedance magnitude measurements were done in triplicate at 51 points within the frequency range utilized in 100 mM MES/1.0 M NaCl, at pH 6.15. Once single strand measurements were completed, the electrodes were exposed to 6 mM target solution and left to react for 1h. After washing with MES buffer to remove excess target strands, impedance measurements were performed again.

E. Analysis

Zfit tool from EC-Lab® software (Bio-Logic, USA) was utilized to interpret the impedance data. Microsoft Excel (Microsoft, Redmond, WA, USA) was used for statistical analysis and graph preparation. Mean values and standard deviations were calculated based on triplicate tests.

III. Results and Discussion

The silver-chloride quasi reference electrode was characterized by Energy Dispersive X-ray Fluorescence Spectroscopy (EDS) and Scanning Electron Microscopy (SEM) to ensure effective silver chloride formation and determine the silver layer thickness. Figure 2 shows EDS and SEM images for the silver-chloride layer. The average silver layer thickness was calculated at 1.38 mm. Subsequent reference electrode stabilization was demonstrated calculating the Au reduction peak potential for the clean voltammograms, which reproducibly appear at 0.63 V.

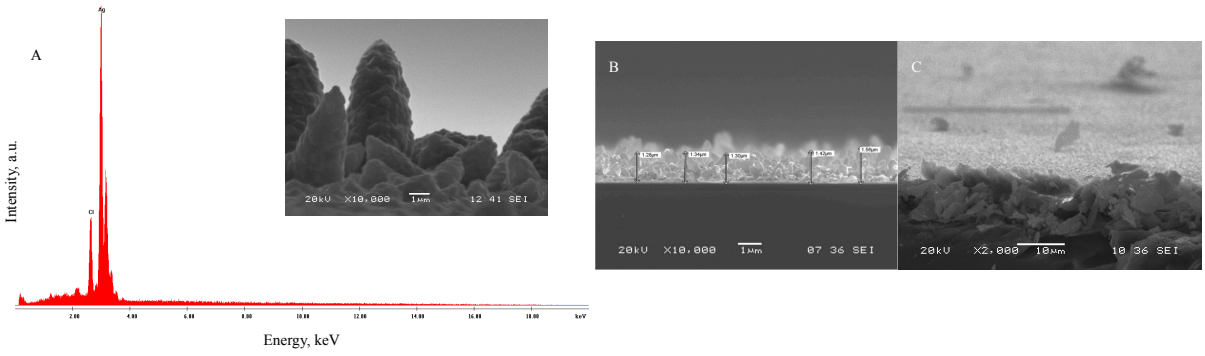

Figure 2. Results of Energy Dispersive X-ray Fluorescence Spectroscopy (EDS) and Scanning Electron Microscopy (SEM) analysis of the silver-silver-chloride reference electrode surface: *Trasnversal view for A) EDS analysis (scale bar= 1 µm) and B) layer thickness calculation (scale bar= 1 µm). Angled view for C) surface imaging (scale bar=10µm).*

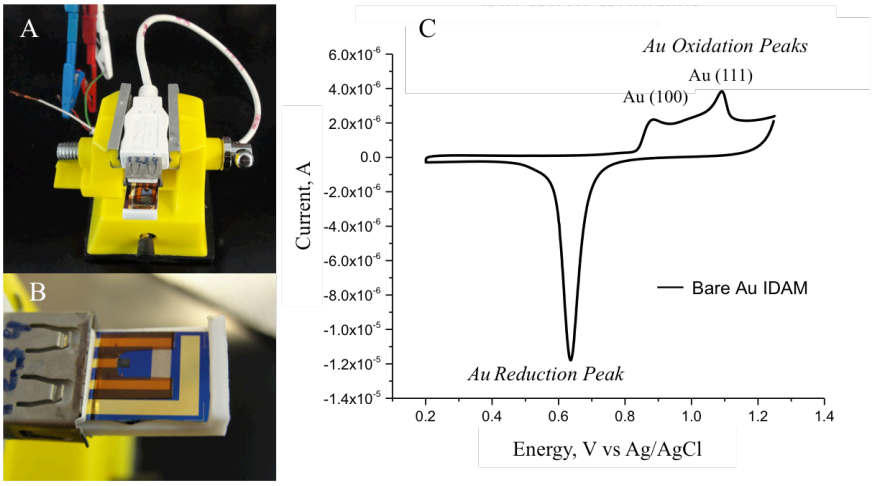

Figure 3. Experimental electrochemical cell arrangement. *A) USB connector cable with microchip plugged in, B) microchip close up and C) characteristic cyclic voltammogram for a clean gold interdigitated microelectrode array in 0.5 M H_2SO_4 from 0.2 V - 1.25 V vs. Ag/AgCl at a scan rate: 50.0 mV/s.*

The microelectrodes were analyzed through cyclic voltammetry to verify and optimize their overall performance as a chip. Cleaning parameters were set to scan the potential between 0.1 V and 1.25 V vs. Ag/AgCl quasi reference at a scan rate of 50.0 mV/s in 0.5 M H_2SO_4. Figure 3 shows the experimental set-up and a typical custom-made clean gold microelectrode cyclic voltammogram, which is characterized by multiple oxidation peaks corresponding to the different rates of gold facets oxidation and a single reduction peak at 0.63 V representative of the silver chloride quasi reference prepared. DNA immobilization and further impedimetric analysis were performed as detailed in the experimental section.

Relating the electrode-solution interface to a capacitor, the electrochemical components of the studied system can be described as an electrical circuit. In means of creating a "plug and play" type of procedure, all EIS measurements were performed in MES buffer at pH 6.15, which is the same buffer utilized for the DNA samples. Our label-free system therefore does not contain any species that can readily perform a redox reaction, which translate to a charge transfer resistance value so large in fact, that within our EIS parameters the diffusion region of the nyquist plot is not reached for the majority of our tests. This leaves us with the simple Randles circuit model consisting only of the electrolyte solution resistance (R_s), charge transfer resistance (R_{ct}) and the double layer capacitance (C_{dl}) as shown in Figure 4(A). However, in a few tests the diffusion zone was briefly reached and, therefore, an additional parameter had to be taken into account: the warburg diffusion (W). An extension of the Randles circuit can integrate W in series with R_{ct}, see Figure 4(B). All impedance data were measured versus open circuit potential (E_{oc}) with the median being 0.05V, and analyzed by fitting the resulting bode plots.

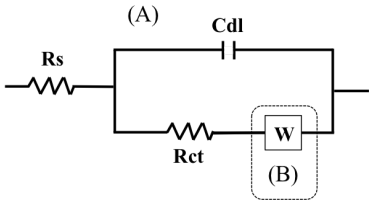

Figure 4. Randles circuit model: *A) simple, and B) extended.*

Direct comparison of capacitance values between electrodes cannot be made due to the lack of reproducibility from the exposed working area since the passivation layer is cut by hand. However, the magnitude of change between electrodes can be compared. The percentage change was calculated as follows:

$$(C_{dl-ssDNA} - C_{dl-DNA+T}/C_{dl-ssDNA}) \cdot 100 \quad (1)$$

Where $C_{dl\text{-}ssDNA}$ and $C_{dl\text{-}DNA+T}$ corresponds to the double layer capacitance value for the B. Anthracis single strand monolayer before and after exposure to target, respectively. Within the data representation options offered by the EIS technique, bode plots were chosen to perform the fittings because they provide a simplified approach for the behavior of the system. Figure 5 displays bode plot spectra before and after DNA complementary target interaction and their respective fittings for a high surface coverage electrode done at an applied potential of 0.3 V vs. E_{oc}

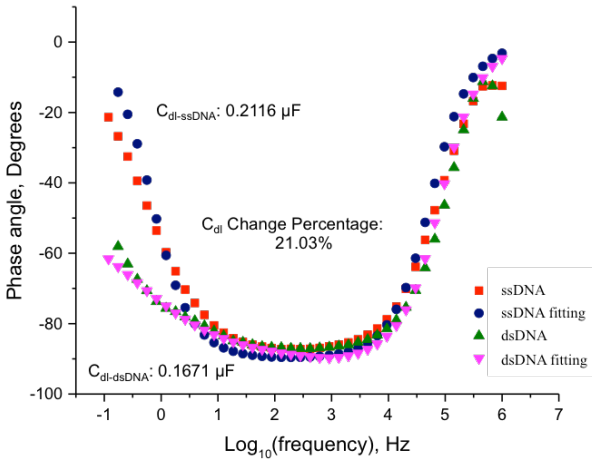

Figure 5: Bode Plot Fittings. *Representative bode plot spectra for a high surface coverage ssDNA monolayer before (red), and after (green) interaction with complementary DNA target and their respective fittings, (blue) and (pink), done at 0.3V vs. E_{oc} applied potential.*

(potential of open circuit or potential of zero charge). For our experimental scheme, when the diffusion zone is not approached, the bode plot generates a symmetric "U" shape and the simplified version of the randles circuit is utilized to perform the calculations. When the diffusion area of the system is reached, the plot begins to distort the "U" shape as the phase angle starts to decrease, making it necesarly to consider W values for proper fitting. Example data set presented in Figure 5 was fitted using the extended randles circuit. A decrese in double layer capacitance was observed upon hybridization, more specifically, 21.0% change. This behavior of decrease in capacitance value upon target strand interaction was consistently observed throughut the experiment.

After all EIS data was fitted and the capacitance values recorded, we proceeded to calculate individual percentage change per electrode. Then, a statistical analysis was performed by calculating the average and standard deviation per sub-division, this is, target strand per applied voltage, per surface coverage. Mean values for all three target interactions per category were graphed, using the calculated standar deviation as error bar. The categories are: (1) Low surface coverage at 0.0 V vs. E_{oc} applied potential, (2) low surface coverage at 0.3 V vs. E_{oc} applied potential, (3) high surface coverage at 0.0 V vs. E_{oc} applied potential and (4) high surface coverage at 0.3 V vs. E_{oc} applied potential. Figure 6 sumarized the experimental data as explained above.

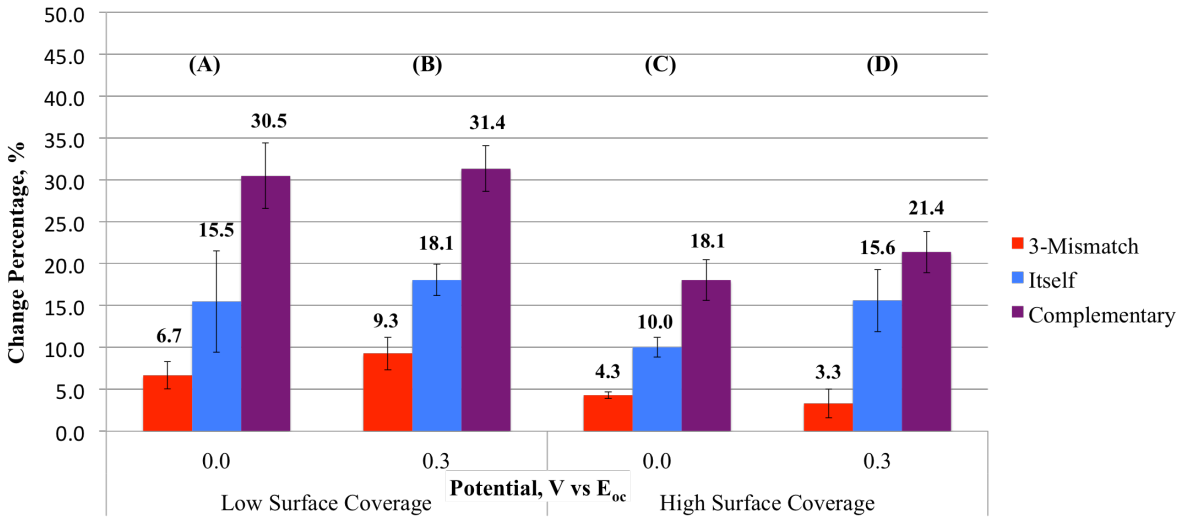

Figure 6. Mean Percentange Difference values for: low (A,B) and high (C,D) ssDNA monolayer surface coverage systems and its interaction with 3-mismatch (red), itslef (blue) and complementary (purple) target strands at 0.0 V and 0.3 V vs. E_{oc} applied potentials.

In the four data sets presented in figure 6, hybridization of DNA by complementary strand exposure produced the higher percentage change values, as expected, being low surface coverage at 0.3V vs. E_{oc} applied potential the highest one with 31.4%. Due to its hairpin nature, the itself oligo consist of complementary bases in the first and last six nucleotides. This means that if the itself strand is rotated (which happends arbitrarily in solution) it can hybridize to the DNA probe at both 3' and 5' terminals but not in between, behaving like a mismatch. 3-mismatch strand

consists of a complementary target with just 3 mismatched bases located throughout the center, however, its interaction with the DNA probe yielded lower percentage change values than itself. This is because the delocalized non-complementary bases in between the 3-mismatch target strand create a more unstable structure than interaction with itself due to intercalation of electrostatic attraction and repulsion forces. Each individual target in both surface coverage systems presented a greater percentage change at the higher applied voltage, with exception of 3-mismatch which showed no pattern. Overall change percentages were of higher magnitude for low surface coverage. This was due to surface over crowding of B. anthracis aptamers in the high surface coverage that prevent effective interaction with target strand due to space hindrance. Low surface coverage at 0.3 V vs. E_{oc} applied potential revealed the best distinction between strand interaction with higher precision, and is therefore the preferred scheme for our future biosensor analysis.

IV. Conclusion

Custom-made interdigitated array microelectrodes were effectively fabricated and employed, which adds an important feature to economic, environmentally friendly and specific biosensors. DNA hybridization by complementary target exposure showed the largest percentage change compared to the single strand DNA monolayer as excepted, followed by interaction with itself while being less affected by the 3-mismatch target. The conditions that showed better distinction between strand interactions with highest reproducibility were low surface coverage at 0.3V vs. E_{oc} applied potential. Overall results showed that double layer capacitance is a measurable property to detect specific DNA sequences. Moreover, our sensor currently meets 7 out of the 11 sensor requirements for space flight use, according to S. L. Bonting, et. al.[21], being (1) accurate, (2) stable, (3) small sized and lightweight, (4) low power consumption and (5) easy to service. Also, once the sensor is prepared, it does not need extra reagents or solvents that otherwise complicate the process, and since all meassurements are presented as percentange change, no need for calibration is required, accounting for the (6) easy calibration, and (7) minimal complexity requirements. As for the four missing, (8) biocompatibility and (9) long lifetime are topics in our current research interest while the (10) ability to operate in micro-gravity and (11) being space-qualified are characteristics that will need further testing and approval with agencies such as the National Aeronautics and Space Administration (NASA).

Acknowledgments

This research was financially supported by NSF-Chemistry Grant No. CHE-1152940 and NASA-MIRO Grant No. NNX10AQ17A. NASA Space Grant Fellowship Grant No. NNX10AM80H supported Nadja E. Solis-Marcano and RISE Fellowship Grant No. 5R25GM061151-14 supported Nadja E. Solis-Marcano and Brismar Pinto-Pacheco. The authors gratefully acknowledge Dr. James J. Watkins, Director of the Center for Hierarchical Manufacturing at University of Massachussets at Amherst, MA, USA, as well as Diana C. Diaz-Cartagena (UPR), Dr. Lisandro Cunci (University of Turabo) and John Nicholson (UMASS) for their contribution in the microelectrode manufacturing process. Special gratitude is also extended to Roberto Martinez (UPR) for assisting with the silver electrodeposition, Myreisa Morales (UPR) and Ángel C. Vélez (UPR) for aiding with various roles.

References

[1]Tongeren, S. P.; Degener, J. E.; Harmsen, H. J. M., "Comparison of three rapid and easy bacterial DNA extraction methods for use with quantitative real-time PCR," *European Journal of Clinical Microbiology & Infectious Diseases* Vol. 30, No. 9, 2011, pp. 1053-1061.

[2]Velusamy, V.; Arshak, K.; Yang, C. F.; Yu, L.; Korostynska, O.; Adley, C., "Comparison between DNA Immobilization Techniques on a Redox Polymer Matrix," *American Journal of Analytical Chemistry,* Vol. 2, No. 3, 2011, pp.4.

[3]Berdat, D.; Marin, A.; Herrera, F.; Gijs, M. A. M., "DNA biosensor using fluorescence microscopy and impedance spectroscopy," *Sensors and Actuators B: Chemical,* Vol. 118, No. 1-2, 2006, pp. 53-59.

[4]Xiao, Y.; Lai, R. Y.; Plaxco, K. W., "Preparation of electrode-immobilized, redox-modified oligonucleotides for electrochemical DNA and aptamer-based sensing," *Nat. Protocols,* Vol. 2, No. 11, 2007, pp. 2875-2880.

[5]Pan, C.; Guo, M.; Nie, Z.; Xiao, X.; Yao, S., "Aptamer-Based Electrochemical Sensor for Label-Free Recognition and Detection of Cancer Cells," *Electroanalysis,* Vol. 21, No. 11, 2009, pp. 1321-1326.

[6]Park, J.-Y.; Park, S.-M., "DNA Hybridization Sensors Based on Electrochemical Impedance Spectroscopy as a Detection Tool," *Sensors,* Vol. 9, No. 12, 2009, pp. 9513.

[7]Sheng, Q.; Liu, R.; Zhang, S.; Zheng, J., "Ultrasensitive electrochemical cocaine biosensor based on reversible DNA nanostructure. *Biosensors and Bioelectronics,"* Vol. 51, 2014, pp. 191-194.

[8]Samitier, R. L. Z. a. M. M. a. J., "Label-free detection of DNA hybridization and single point mutations in a nano-gap biosensor. *Nanotechnology,"* Vol. 25, No. 10, 2014, pp. 105501.

[9]Santiago-Rodríguez, L.; Sánchez-Pomales, G.; Cabrera, C. R., "Single-Walled Carbon Nanotubes Modified Gold Electrodes as an Impedimetric DNA Sensor," *Electroanalysis,* Vol. 22, No. 4, 2010, pp. 399-405.

[10]Bravo-Anaya, L. M.; Macías, E. R.; Ramos, F. C.; Fernández, V. V. A.; Casillas, N.; Soltero, J. F. A.; Larios-Durán, E. R., "DNA Conformational Transitions at Different Concentrations and Temperatures Monitored by EIS," *ECS Electrochemistry Letters,* Vol. 1, No. 2, 2012, pp. G1-G3.

[11]Lum, J.; Wang, R.; Hargis, B.; Tung, S.; Bottje, W.; Lu, H.; Li, Y., "An Impedance Aptasensor with Microfluidic Chips for Specific Detection of H5N1 Avian Influenza Virus," *Sensors,* Vol. 15, No. 8, 2015, pp. 18565.

[12]Rivera-Gandía, J.; del Mar Maldonado, M.; De La Torre-Meléndez, Y.; Ortiz-Quiles, E. O.; Vargas-Barbosa, N. M.; Cabrera, C. R., "Electrochemical Capacitance DNA Sensing at Hairpin-Modified Au Electrodes," *Journal of Sensors***,** Vol. 2011, 2011.

[13]Guiducci, C.; Stagni, C.; Zuccheri, G.; Bogliolo, A.; Benini, L.; Samori, B.; Ricco, B. In "A Biosensor for Direct Detection of DNA Sequences Based on Capacitance Measurements," *Proceeding of the 32nd European Solid State Device Conference,* 2002, pp. 479-482.

[14]Altintas, Z.; Kallempudi, S. S.; Gurbuz, Y., "Gold nanoparticle modified capacitive sensor platform for multiple marker detection," *Talanta,* Vol. 118, 2014, pp. 270-276.

[15]Akbulut, A.; Akbulut, H.; Özgüler, M. g.; Inci, N.; Yalçin, i., "Gastrointestinal Anthrax: A Case and Review of Literature," *Advances in Infectious Diseases*, Vol. 2, No. 3, 2012, pp. 5.

[16]Kalb, S.; Boyer, A.; Barr, J., "Mass Spectrometric Detection of Bacterial Protein Toxins and Their Enzymatic Activity," *Toxins,* Vol. 7. No. 9, 2015, pp. 3497.

[17]Hansen, W. L. J.; Bruggeman, C. A.; Wolffs, P. F. G., "Pre-analytical Sample Treatment and DNA Extraction Protocols for the Detection of Bacterial Pathogens from Whole Blood," In *PCR Detection of Microbial Pathogens*, Wilks, M., Ed. Humana Press: Totowa, NJ, 2013; pp 81-90.

[18]Barken, K. B.; Haagensen, J. A. J.; Tolker-Nielsen, T., "Advances in nucleic acid-based diagnostics of bacterial infections," *Clinica Chimica Acta,* Vol. 384, No. 1–2, 2007, pp. 1-11.

[19]Schlesinger, M., "Electroless and Electrodeposition of Silver," In *Modern Electroplating*, John Wiley & Sons, Inc.: 2010; pp 131-138.

[20]Polk, B. J.; Stelzenmuller, A.; Mijares, G.; MacCrehan, W.; Gaitan, M., "Ag/AgCl microelectrodes with improved stability for microfluidics," *Sensors and Actuators B: Chemical,* Vol. 114, No. 1, 2006, pp. 239-247.

[21]Bonting, S. L., "Utilization of biosensors and chemical sensors for space applications," *Biosensors and Bioelectronics,* Vol. 7, No. 8, 1992, pp. 535-548.